Amino Acids (2014) 46:2355–2364
DOI 10.1007/s00726-014-1788-x

ORIGINAL ARTICLE

A direct comparison of tumor angiogenesis with ^{68}Ga-labeled NGR and RGD peptides in HT-1080 tumor xenografts using microPET imaging

Yahui Shao · Wansheng Liang · Fei Kang · Weidong Yang · Xiaowei Ma · Guiyu Li · Shu Zong · Kai Chen · Jing Wang

Received: 26 March 2014 / Accepted: 13 June 2014 / Published online: 3 July 2014

Abstract Peptides containing asparagine-glycine-arginine (NGR) and arginine-glycine-aspartic acid (RGD) sequence are being developed for tumor angiogenesis-targeted imaging and therapy. The aim of this study was to compare the efficacy of NGR- and RGD-based probes for imaging tumor angiogenesis in HT-1080 tumor xenografts. Two PET probes, ^{68}Ga-NOTA-G_3-NGR2 and ^{68}Ga-NOTA-G_3-RGD2, were successfully prepared. In vitro stability, partition coefficient, tumor cell binding, as well as in vivo biodistribution properties were also analyzed for both PET probes. The results revealed that the two probes were both hydrophilic and stable in vitro and in vivo, and they were excreted predominately and rapidly through the kidneys. For both probes, the higher tumor uptake and lower accumulation in vital organs were determined. No significant difference between two probes was observed in terms of tumor uptake and the in vivo biodistribution properties. We concluded that these two probes are promising in tumor angiogenesis imaging. ^{68}Ga-NOTA-G_3-NGR2 has the potential as an alternative for PET imaging in patients with fibrosarcoma, and it may offer an opportunity to noninvasively monitor CD13-targeted therapy.

Keywords MicroPET imaging · NGR · RGD · CD13 · Integrin · Tumor angiogenesis · ^{68}Ga labeling

Y. Shao and W. Liang contributed equally to this work.

Electronic supplementary material The online version of this article (doi:10.1007/s00726-014-1788-x) contains supplementary material, which is available to authorized users.

Y. Shao · F. Kang · W. Yang · X. Ma · G. Li · S. Zong · J. Wang (✉)
Department of Nuclear Medicine, Xijing Hospital, The Fourth Military Medical University, 15 Changle West Road, Xi'an 710032, Shaanxi, China
e-mail: wangjing@fmmu.edu.cn

Y. Shao
Department of Nuclear Medicine, General Hospital of Jinan Military Area Command of the Chinese People's Liberation Army, Jinan 250031, Shandong, China

W. Liang
Department of Nuclear Medicine, Lanzhou General Hospital of Lanzhou Military Area Command of the Chinese People's Liberation Army, Lanzhou 730050, Gansu, China

K. Chen (✉)
Department of Radiology, Molecular Imaging Center, Keck School of Medicine, University of Southern California, 2250 Alcazar Street, CSC103, Los Angeles, CA 90033, USA
e-mail: chenkai@usc.edu

Introduction

It is well known that tumor growth and metastasis are angiogenesis-dependent. Angiogenesis is one of the most attractive targets for anticancer therapies and imaging in preclinical and clinical studies (Carmeliet and Jain 2000). Biological markers, which are selectively expressed at high levels in the endothelial cells of proliferating vessels and tumor cells in response to angiogenic signals, can be targeted for early detection and anticancer therapy (Jain et al. 2009; Ribatti et al. 2012). For instance, aminopeptidase N (APN/CD13) has multiple functions associated with the progression of malignancy, such as facilitating the invasion of endothelial cells into the tumor stroma, and enhancing the invasiveness of tumor cells, proliferation, secretion, and angiogenesis (Bhagwat et al. 2001; Wickstrom et al. 2011). Pasqualini et al. (1995, 2000) performed a series of studies demonstrating that phages expressing the asparagine-glycine-arginine (NGR) motif have strong binding affinity

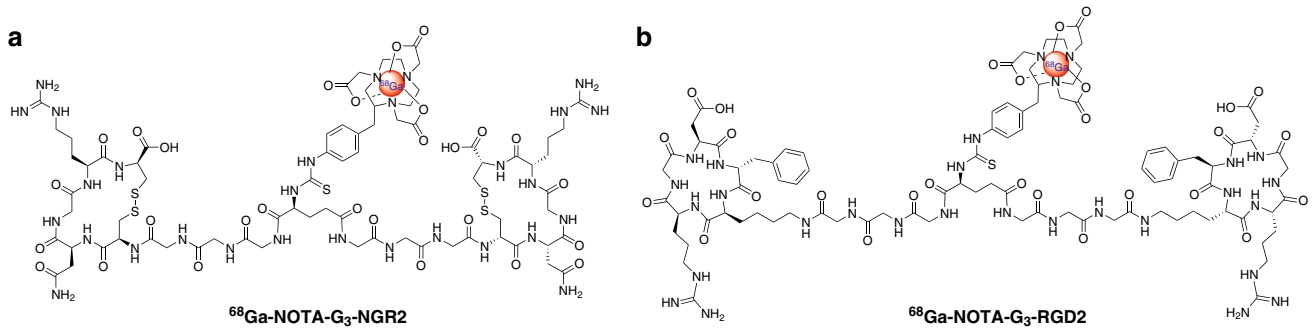

Fig. 1 Chemical structures of ^{68}Ga-NOTA-G_3-NGR2 (**a**) and ^{68}Ga-NOTA-G_3-RGD2 (**b**)

to neovascular tissue via the principal APN receptor. Peptides containing the NGR motif have been used as a homing agent for delivery of therapeutics, chemicals, peptides, cytokines, liposomes, and polymeric micelles to activated tumor neovascular tissue to enhance therapeutic efficacy and reduce systemic toxicity (Wang et al. 2012).

Oliveira et al. (2012) reported that the performance of a ^{99m}Tc-labeled arginine-glycine-aspartic acid (RGD) tracer was better than the NGR tracer in terms of human melanoma uptake. However, compared with RGD, Arap et al. (1998) reported that the tumor selectivity of NGR peptide was three-fold higher than RGD peptide, and that NGR peptide exhibited the greatest tumor selectivity of all the peptides tested from a phage peptide library. Apparently, the observations of Oliveira et al. differ from the in vivo phage display experiment.

Over the past decade, RGD peptides have been explored extensively for the tumor imaging. A variety of RGD-based radiopharmaceuticals have been used to image various tumors (Li et al. 2008; Liu et al. 2009, 2012), and some RGD-containing probes are currently in clinical studies (Beer et al. 2008). In terms of the in vivo phage display results, NGR-based probes are very promising for imaging tumor angiogenesis. However, as compared to RGD-containing probes, NGR peptides remained under-investigated. Most imaging studies using NGR-based probes focused on optical imaging with NGR-conjugated fluorescent dyes to assess the mechanisms of cellular uptake, monitor drug delivery, and characterize tumor responses at the cellular levels (Dirksen et al. 2004; Negussie et al. 2010).

Until recently, several radiolabeled NGR peptides have been reported (Chen et al. 2013; Faintuch et al. 2014; Jiang et al. 2012; Ma et al. 2013; Zhang et al. 2014), these studies indicated that a NGR-containing peptide can serve as an ideal candidate for targeted angiogenesis imaging in various tumors. For example, we recently synthesized two 1,4,7,10-tetraazacyclododecane-*N*,*N*′,*N*″,*N*‴-tetraacetic acid (DOTA)-conjugated cyclic NGR peptides, monomer and dimer, and labeled them with ^{64}Cu for positron emission tomography (PET) imaging (Chen et al. 2013). These peptides showed excellent tumor uptake in CD13-positive HT-1080 tumor xenografts. Overall, the preclinical results of radiolabeled NGR-containing peptides are quite promising, which may lead to future clinical applications.

Although radiolabeled NGR- and RGD-containing peptides can be used for tumor angiogenesis imaging, to the best of our knowledge, a direct comparison of in vivo imaging effectiveness between NGR- and RGD-containing peptide has not been pursued in depth. A question, regarding the preference of a radiolabeled probe (either NGR- or RGD-based probe) for the noninvasive angiogenesis imaging in tumors which are selectively co-expressed CD13 and $\alpha_v\beta_3/\alpha_v\beta_5$ integrin, remains unknown. A direct comparative preclinical study between radiolabeled NGR- and RGD-containing probes is therefore highly demanded.

To this end, we constructed a new NGR peptide, 1,4,7-triazacyclononane-*N*,*N*′,*N*″-triacetic acid (NOTA)-conjugated dimeric Gly_3-CNGRC cyclic peptide (NOTA-G_3-NGR2; Fig. 1), and labeled with ^{68}Ga for microPET imaging in subcutaneous mouse HT-1080 fibrosarcoma xenografts, which co-expressed high levels of CD13 (Chen et al. 2013) and $\alpha_v\beta_3/\alpha_v\beta_5$ integrin (Kim et al. 2011). A ^{68}Ga-labeled NOTA-G_3-RGD2 peptide was used for a side by side comparison to determine the ability of noninvasive angiogenesis PET imaging in HT-1080 tumor xenografts.

Experimental section

General

All commercially obtained chemicals were of analytical grade and used without further purification. Cyclic NGR peptide [GGGCNGRC; disulfide Cys:Cys = 4-8] was purchased from CS Bio Company, Inc. (Menlo Park, CA, USA). The dimeric peptide E[Gly_3-c(CNGRC)]$_2$ was synthesized as described previously (Chen et al. 2013). *p*-SCN-Bn-NOTA (Macrocyclics Inc., Dallas, TX, USA)

was conjugated with the dimeric NGR peptides via forming stable thiourea bonds. ^{68}Ga was obtained from a ^{68}Ge/^{68}Ga generator (produced by ITG Isotope Technologies Garching GmbH, Germany) and eluted with 4 mL of 0.05 M HCl. The semi-preparative high-performance liquid chromatography for peptide analysis was performed as described previously (Chen et al. 2013). Mass spectra were obtained using a Thermo-Electron Finnigan LTQ mass spectrometer equipped with an electrospray ionization source (Thermo Scientific, Waltham, MA, USA). Radiochemical purity (RCP) was measured by radio-TLC which was performed on silica gel-coated plastic sheets (Polygram SIL G, Macherey–Nagel) with sodium citrate (0.1 M, pH = 5). The results were read by Mini-scan (Bioscan, Washington, DC, USA) and Allchrom Plus software. The NOTA-G_3-RGD2 peptide was a generous gift from the National Institute of Biomedical Imaging and Bioengineering.

^{68}Ga labeling and formulation

NOTA-G_3-NGR2 and NOTA-G_3-RGD2 peptides were labeled with ^{68}Ga as described previously (Liu et al. 2009), with slight modifications. Briefly, peptides (15 nmol) were dissolved in 500 μL of 0.1 M sodium acetate buffer and incubated with 1,295 MBq of ^{68}Ga for 10 min at 42 °C. Then 30 μL of 1.25 M NaOAc buffer was added, and samples were then fixed on a Sep-Pak C18 SPE cartridge (Waters Corporation, Vienna, Austria) and washed with 5 mL water. ^{68}Ga-labeled peptides were eluted with 2 mL of 50 % ethanol saline solution, and concentrated by rotary evaporation. The product was dissolved in water for injection, and passed through a 0.22 μm Millipore filter into a sterile dosing vial for use in subsequent experiments.

Partition coefficient

The partition coefficient was determined by measuring the distribution of radioactivity in octanol and PBS. Approximately 5 KBq ^{68}Ga-NOTA-G_3-RGD2 or ^{68}Ga-NOTA-G_3-NGR2 was added to a vial containing 0.5 mL of octanol and 0.5 mL of PBS (pH 7.4), and vortexed vigorously for 15 min. Subsequently, the mixture was centrifuged at 12,500 rpm for 5 min. Aliquots of the aqueous and octanol layers were collected, measured in a gamma counter (Beijing PET CO., Ltd., China), and log$P$ values were calculated (mean of $n = 5$).

Determination of in vitro stability

The stability of ^{68}Ga labeled peptides was assessed by mixing 0.1 mL (3.7 MBq) of ^{68}Ga-NOTA-G_3-RGD2 or ^{68}Ga-NOTA-G_3-NGR2 solution with 0.9 mL of fresh human serum at 37 °C or 0.1 mL of the saline at room temperature with gentle shaking. The RCP was measured at various time points (1, 2, and 4 h).

Cell culture and animal model

The HT-1080 human fibrosarcoma and HT-29 human colon adenocarcinoma cell lines were maintained in high glucose DMEM culture medium supplemented with 10 % (v/v) fetal bovine serum (Gibco, USA), 1 % L-glutamine, and 1 % mycillin (Beyotime, China) in a humidified atmosphere of 5 % CO_2 at 37 °C. The cells were detached from the culture flasks using trypsin—ethylenediaminetetraacetic acid (EDTA), and then resuspended in medium for implantation. Using female nude BALB/c mice (4–6 weeks old, weighing 20–25 g), HT-1080 and HT-29 tumor xenografts were established by subcutaneously injecting 0.1 mL of tumor cell suspension (5×10^6 cells) into the right upper flank. When tumors reached 500–1,000 mm^3 in volume, mice were used for biodistribution and microPET imaging studies. All animal studies were approved by the Clinical Center at the FMMU.

Cell binding assay

In vitro integrin and CD13 receptor binding affinity and specificity of NOTA-G_3-RGD2 and NOTA-G_3-NGR2 in HT-1080 cells were assessed via competitive cell-binding assay. ^{125}I-labeled linear NGR peptide (sequence H-Tyr-Gly-Gly-Cys-Asn-Gly-Arg-Cys-OH) was prepared using the iodogen method and used as the radioligand for CD13, whereas ^{125}I-echistatin (Biotrend Chemikalien GmbH, Köln, Germany) was used as the radioligand for integrin. The cold peptides concentrations were at a range from 10^{-12} to 10^{-5} M. The IC_{50} (50 % inhibitory concentration) values were obtained by fitting the data using nonlinear regression with GraphPad Prism (GraphPad Software, San Diego, CA, USA). Experiments were performed in triplicate.

MicroPET imaging

MicroPET studies were performed to compare the in vivo uptake characteristics of the two probes in HT-1080 (CD13+, integrin $\alpha_v\beta_3$+) and HT-29 (CD13−, integrin $\alpha_v\beta_3$−) bearing nude mice. Mice were intravenously injected with ~3.7 MBq of ^{68}Ga-NOTA-G_3-RGD2 or ^{68}Ga-NOTA-G_3-NGR2 on two consecutive days under isoflurane anesthesia ($n = 5$/group). Ten-minute static scans and helical CT images were acquired at 0.5, 1, and 2 h pi using Mediso NanoPET/CT scanner (Mediso, Budapest, Hungary). PET and CT fused images were obtained using the automatic fusion feature of the image fusion software (Mediso, Budapest, Hungary). ^{18}F-FDG microPET images were acquired before ^{68}Ga-NOTA-G_3-RGD2 or ^{68}Ga-NOTA-G_3-NGR2 scanning.

For the blocking experiment, mice bearing HT-1080 tumor xenografts (n = 5/group) were co-injected with 20 mg/kg NOTA-G_3-RGD2 or NOTA-G_3-NGR2, and ~3.7 MBq of ^{68}Ga-labeled probes. The accumulation of radioactivity in the tumor was obtained from the mean value within the multiple regions of interest and converted to % ID/g, and then calculated the tumor to non-tumor (T/NT) ratio.

Biodistribution studies

Nude mice bearing human HT-1080 tumor xenografts were injected with ^{68}Ga-NOTA-G_3-RGD2 or ^{68}Ga-NOTA-G_3-NGR2 peptide (370 kBq/animal) via the tail vein. The mice were sacrificed by cervical dislocation at 60 min pi and dissected. Blood, tumor, major organs (heart, stomach, lung, spleen, liver, brain, kidneys, intestine, and bone), and muscle were harvested, weighed, and measured radioactivity in a gamma counter. Decay-corrected mean uptake (% ID/g) for a group of animals was calculated with standard deviations (mean ± SD, n = 5/group).

Statistical analysis

Quantitative data were expressed as mean ± SD. Means were compared using one-way ANOVA and Student's t test. P values <0.05 were considered to be statistically significant.

Results

Chemistry and radiochemistry

Through conjugation of E[Gly_3-c(NGR)]$_2$ and p-SCN-Bn-NOTA, NOTA-G_3-NGR2 was achieved in a yield of 62 %. The synthetic scheme of ^{68}Ga-NOTA-G_3-NGR2 is shown in Fig S1. The resulting peptide was then purified using HPLC and characterized by mass spectrometry (ESI–MS). The electrospray ionization mass spectra of NOTA-G_3-NGR2 was determined to be $[M + 2H]^{2+}$ m/z = 1,002.75 (Fig S2). The HPLC purity of the peptide used in subsequent experiments was >95 %. All labeling procedures were performed within 30 min. The decay-corrected yield ranged from 95 to 98 %, and the radiochemical purity was >99 % after purification (Fig S3). The specific activity of purified ^{68}Ga-NOTA-G_3-RGD2 and ^{68}Ga-NOTA-G_3-NGR2 was 13.47–16.44 MBq/nmol. The ^{68}Ga-labeled probes were used immediately after formulation. The chemical structures of ^{68}Ga-NOTA-G_3-NGR2 and ^{68}Ga-NOTA-G_3-RGD2 are shown in Fig. 1.

Log P value

The partition coefficient (log$P$) of ^{68}Ga-NOTA-G_3-RGD2 and ^{68}Ga-NOTA-G_3-NGR2 were determined to be -3.01 ± 0.17 and -2.76 ± 0.20, respectively, suggesting that both ^{68}Ga-labeled peptides are hydrophilic.

In vitro stability

The in vitro stability of ^{68}Ga-NOTA-G_3-NGR2 and ^{68}Ga-NOTA-G_3-RGD2 in PBS (pH 7.4) at room temperature and fresh human serum at 37 °C are shown in Fig. 2. After 4 h of incubation, more than 97 % of ^{68}Ga-NOTA-G_3-NGR2 and more than 96 % of ^{68}Ga-NOTA-G_3-RGD2 remained intact in PBS as well as human serum.

Cell-based binding assay

HT-1080 cells were used to measure the in vitro binding affinity of NOTA-G_3-RGD2 to integrin and NOTA-G_3-NGR2 to CD13 using competitive cell-binding assays. Increasing amounts of NOTA-G_3-RGD2 or NOTA-G_3-NGR2 were able to fully suppress the binding of ^{125}I-echistatin to integrin or ^{125}I-NGR to CD13 in a concentration-dependent manner. Western blot results of CD13 and integrin α_v expression in

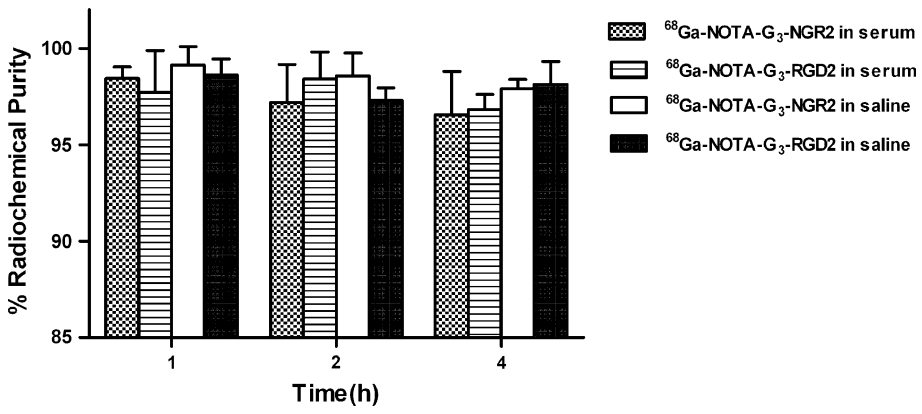

Fig. 2 In vitro stability of ^{68}Ga-NOTA-G_3-RGD2 and ^{68}Ga-NOTA-G_3-NGR2 in saline at room temperature and human serum at 37 °C for 1, 2, and 4 h

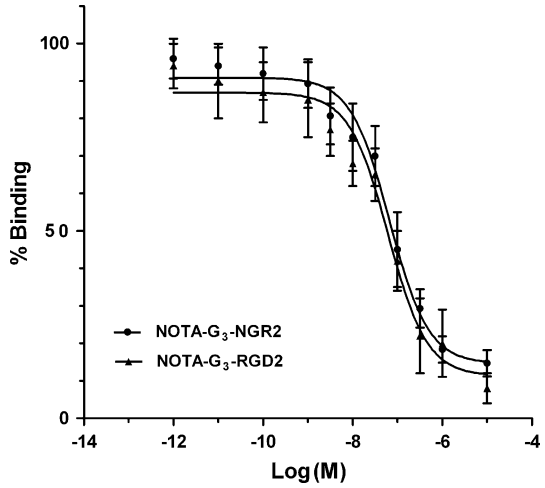

Fig. 3 In vitro inhibition of the binding of NOTA-G_3-NGR2 and NOTA-G_3-RGD2 to CD13 and integrin on HT-1080 cells by ^{125}I-NGR and ^{125}I-echistatin, respectively. The IC_{50} values of NOTA-G_3-RGD2 and NOTA-G_3-NGR2 were 54.54 ± 6.42 and 65.99 ± 1.59 nM, respectively ($n = 3$); ($F = 3.883$, $P > 0.05$)

HT-1080 and HT-29 cells are shown in Fig S4, respectively. The data of cell uptake and efflux study are shown in Fig S5. The binding curves are shown in Fig. 3. The IC_{50} values of NOTA-G_3-NGR2 and NOTA-G_3-RGD2 were 65.99 ± 1.59 and 54.54 ± 6.42 nM, respectively ($F = 3.883$, $P > 0.05$).

MicroPET imaging

Static microPET scans were performed at multiple time points (0.5, 1, and 2 h) in HT-1080 and HT-29 tumor xenografts (n = 5/group). The HT-1080 tumor xenografts were clearly visible with good tumor-to-background contrast for both tracers (^{68}Ga-NOTA-G_3-RGD2 and ^{68}Ga-NOTA-G_3-NGR2) at all time points. For ^{68}Ga-NOTA-G_3-NGR2, tumor uptake was 6.42 ± 2.21, 5.43 ± 2.76, and 4.02 ± 2.03 % ID/g, whereas for ^{68}Ga-NOTA-G_3-RGD2, tumor uptake was 7.84 ± 1.94, 6.26 ± 1.63, and 5.13 ± 1.88 % ID/g at 0.5, 1, and 2 h pi, respectively. There was no significant difference in tumor uptake of the two probes in HT-1080 tumor xenografts at all measured time points ($P > 0.05$). For CD13 and integrin $\alpha_v\beta_3$ negative HT-29 tumor model, both probes exhibited minimal tumor uptake. Representative decay-corrected coronal image slices are shown in Fig. 4. H&E and indirect immunohistochemistry of CD13 receptor/integrin α_v of HT-1080 tumor xenografts are shown in Fig S6. MicroPET images of ^{18}F-FDG are shown in Fig S7.

Co-injection of 20 mg/kg NOTA-G_3-RGD2 or NOTA-G_3-NGR2 peptide led to significant tumor uptake reductions. The tumor uptake of ^{68}Ga-NOTA-G_3-NGR2 was calculated to be 1.43 ± 0.44 % ID/g after co-injection with NOTA-G_3-NGR2 at 1 h pi. Similarly, the uptake of ^{68}Ga-NOTA-G_3-RGD2 was

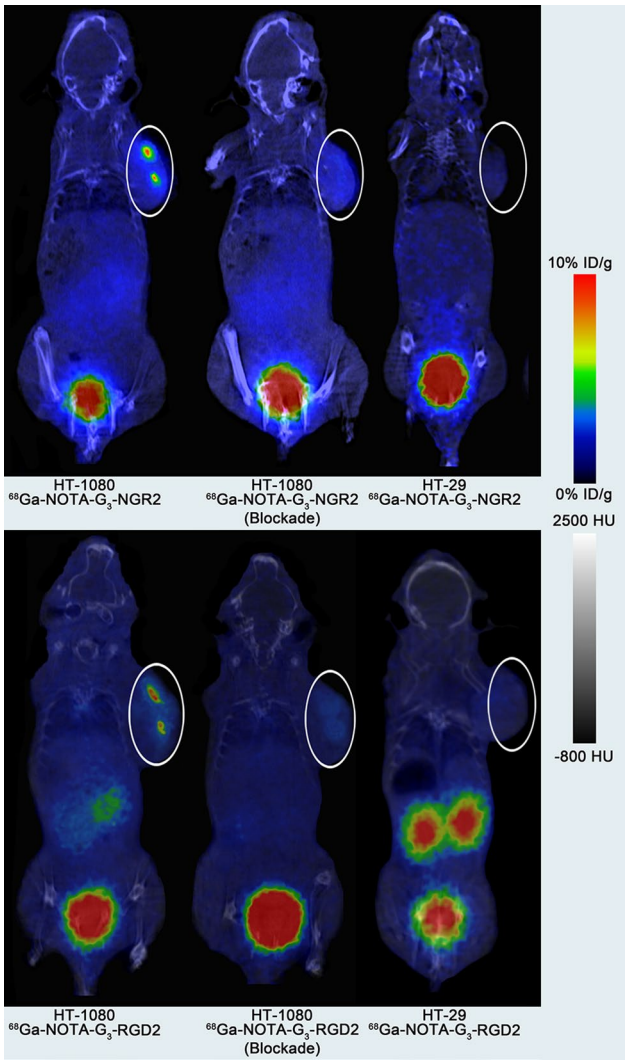

Fig. 4 Representative decay-corrected coronal image slices of mice bearing HT-1080 or HT-29 tumors after intravenous administration of ^{68}Ga-NOTA-G_3-NGR2 or ^{68}Ga-NOTA-G_3-RGD2 at 1 h pi, and the co-injection of non-labeled NOTA-G_3-NGR2 or NOTA-G_3-RGD2 as blocking agents. Tumors are indicated using *circles*

calculated to be 1.28 ± 0.65 % ID/g after co-injection with NOTA-G_3-RGD2 at 1 h pi vs. 6.26 ± 1.63 % ID/g without blocking. There was no significant difference in the targeting specificity of the two probes ($P > 0.05$) (Fig. 5a, c). Both probes cleared rapidly from the blood, and were excreted mainly through the kidneys. The accumulation of the probes in most other organs was very low (Fig. 5c). A one-sample t test revealed that the liver accumulation of the two probes was significantly lower than that of ^{64}Cu-DOTA-NGR2 (Chen et al. 2013) ($P < 0.01$) at 1 h pi.

The T/NT ratios of the two probes at 1 h were calculated and compared in Fig. 5b. The ratio of HT-1080 tumor xenografts uptake to muscle, liver, and kidney and blood accumulation at 1 h pi was calculated to be 7.76 ± 1.16,

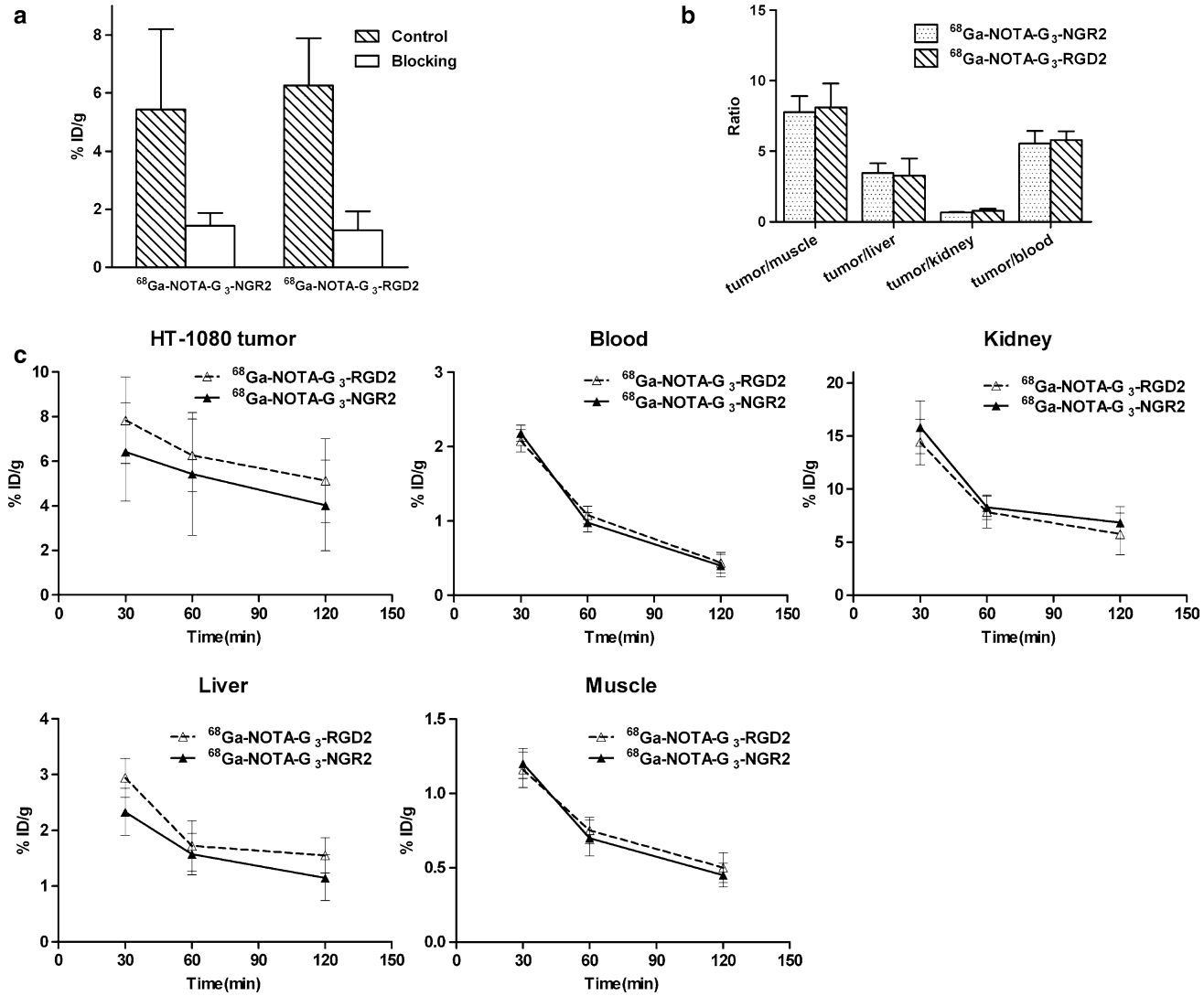

Fig. 5 **a** The uptake of ^{68}Ga-NOTA-G$_3$-RGD2 or ^{68}Ga-NOTA-G$_3$-NGR2 peptide with or without non-labeled NOTA-G$_3$-RGD2 or NOTA-G$_3$-NGR2 in HT-1080 tumor-bearing mice at 1 h pi was quantified using microPET imaging. There was no significant difference in the targeting specificity of the two probes ($P > 0.05$). **b** The ratio of HT-1080 tumor uptake to muscle, liver, kidney, and blood at 1 h pi quantified by micro-PET imaging in HT-1080 tumor bearing mice. There was no significant difference in any ratios between the two probes ($P > 0.05$). **c** Decay-corrected radioactivity accumulation from quantitative microPET imaging analysis of the tumors, blood, kidney, liver, and muscle of HT-1080 tumor-bearing mice at 30, 60, and 120 min after injection with 3.7 MBq of ^{68}Ga-NOTA-G$_3$-RGD2 or ^{68}Ga-NOTA-G$_3$-NGR2

3.47 ± 0.69, 0.66 ± 0.04, and 5.54 ± 0.89 for ^{68}Ga-NOTA-G$_3$-NGR2, respectively; the corresponding values for ^{68}Ga-NOTA-G$_3$-RGD2 were 8.12 ± 1.69, 3.26 ± 1.23, 0.78 ± 0.14, and 5.79 ± 0.61. There were no significant differences in all these ratios between ^{68}Ga-NOTA-G$_3$-NGR2 and ^{68}Ga-NOTA-G$_3$-RGD2 ($P > 0.05$).

Biodistribution studies

Ex vivo biodistribution studies for the two probes were performed at 1 h pi using nude mice bearing HT-1080 tumor xenografts (Fig. 6). The absolute tumor uptake of ^{68}Ga-NOTA-G$_3$-NGR2 and ^{68}Ga-NOTA-G$_3$-RGD2 was comparable ($P > 0.05$). At 1 h pi, the HT-1080 tumor uptake of ^{68}Ga-NOTA-G$_3$-RGD2 and ^{68}Ga-NOTA-G$_3$-NGR2 reached 6.89 ± 2.34 and 5.18 ± 1.06 % ID/g, respectively. Both probes exhibited minimal uptake in most organs, except for a high accumulation and retention in the kidneys. These uptake values were consistent with those calculated from microPET imaging.

Discussion

PET-CT imaging applications are playing an increasing role in both preclinical and clinical studies. It is

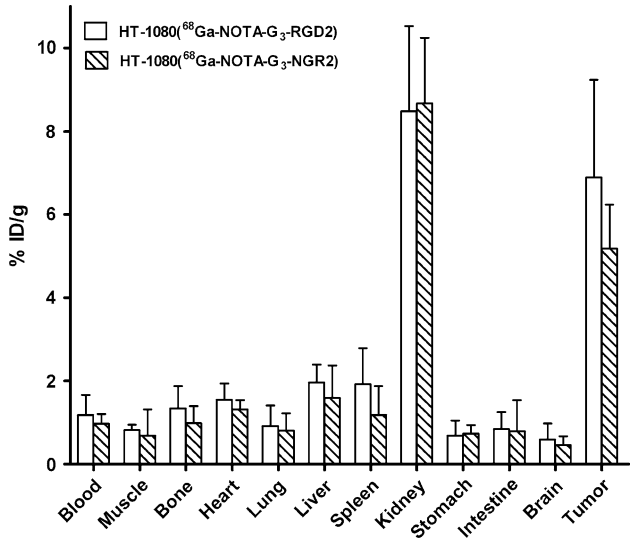

Fig. 6 Decay-corrected biodistribution of ^{68}Ga-NOTA-G$_3$-RGD2 and ^{68}Ga-NOTA-G$_3$-NGR2 at 1 h pi in HT-1080 tumor bearing mice ($n = 5$/group, mean ± SD)

well-documented that ^{18}F-FDG, a most commonly used PET radiopharmaceutical, is not a target-specific probe. Therefore, it may not be suitable to assess angiogenesis in malignancies directly. After labeling with positron-emitting radionuclides, biologically active molecules which can specifically recognize the receptors overexpressed in tumor tissue can be used efficiently for tumor imaging. Selectively targeting biomarkers can themselves serve as analytical tools before commencing expensive therapies (Goggi et al. 2013; Josephson and Rudin 2013). These images might also reveal the therapeutic response in preclinical and clinical studies at the early stages. In addition, rationally designed precursors could be labeled with different radionuclides for diagnosis and therapy in nuclear medicine. The co-development of diagnostic and therapeutic agents may allow the more efficient identification of patients that are likely to respond to expensive targeted therapies. The aim of our study was to select appropriate probes for imaging angiogenesis in HT-1080 tumor xenografts. To this end, we prepared ^{68}Ga-NOTA-G$_3$-NGR2 and compared its tumor targeting efficacy with ^{68}Ga-NOTA-G$_3$-RGD2 by using microPET imaging.

As compared to the commonly used positron-emitting nuclides, such as ^{18}F, ^{11}C, ^{13}N, ^{15}O, and ^{64}Cu, ^{68}Ga has certain advantages. ^{68}Ga is a cost-effective radioisotope that can be obtained easily from a ^{68}Ge/^{68}Ga generator, allowing clinical studies to be performed without an on-site cyclotron. It has an ideal half-life (67.7 min), and its positron abundance (89 %) is suitable for PET imaging (Riss et al. 2011). Compared with ^{11}C and ^{18}F labeling procedures, the ^{68}Ga labeling is relatively simple, efficient, reproducible, and affordable. A kit formulation can be even set up, which greatly facilitates clinical applications (Li et al. 2008).

In terms of radiolabeling, ^{68}Ga has to be complexed with bifunctional chelators (Roesch and Riss 2010), such as NOTA and DOTA. Compared with DOTA, NOTA has the following advantages for $^{68}Ga^{3+}$ labeling. Firstly, the size of the central cavity in NOTA is smaller than that in DOTA, which is more suitable for $^{68}Ga^{3+}$. Therefore, ^{68}Ga-NOTA complexe is relatively more stable than ^{68}Ga-DOTA complexe. The Ga-NOTA complexe is even stable in 6 M nitric acid over a period of 6 months (Parker 1990). Secondly, the slow complexation kinetics of DOTA requires longer reaction times and higher temperatures, whereas NOTA can be complexed with ^{68}Ga nearly quantitatively at room temperature within shorter incubation time. Taken together, NOTA is a better choice for ^{68}Ga labeling to form a stable complex (Correia et al. 2011; Zeglis and Lewis 2011). In addition, compared with other radiometal-DOTA complexes, such as ^{64}Cu-DOTA, ^{68}Ga-NOTA complex is relatively more stable. ^{64}Cu-DOTA complex often result in increased transchelation in the liver, causing an unnecessary high hepatic uptake of ^{64}Cu. In contrast, ^{68}Ga-NOTA complexes can be less transchelated. Our data in this study were consistent with these findings. For instance, the liver uptake of ^{68}Ga-NOTA-G$_3$-NGR2 and ^{68}Ga-NOTA-G$_3$-RGD2 was 2.33 ± 0.42 and 2.94 ± 0.35 % ID/g at 0.5 h pi, respectively, which was lower than that of our previously reported ^{64}Cu-DOTA-NGR2 (Chen et al. 2013) ($P < 0.05$). The low liver and vital organs uptake, and rapid renal excretion resulted in reduced radiation doses in the major organs, leading to favorable translation into the clinic.

One challenge of using an active targeting strategy is the low degree or heterogeneity of receptor expression in different tumor cells (Shamay et al. 2014). It was reported that the construction and blood flow of tumor vessels are disordered and varying, and that biomarkers of tumor vessels are heterogeneous and can be absent or barely detectable in mature vessels (Carmeliet and Jain 2000). Several studies reported that the relationship between the tumor uptake of RGD peptides and integrin $\alpha_v\beta_3$ expression in some subcutaneous tumor-bearing models was linearly dependent (Haubner et al. 2005; Schnell et al. 2009), and tumor blood vessel density was also correlated with tumor uptake. Although HT-1080 tumor xenografts co-express CD13 and $\alpha_v\beta_3/\alpha_v\beta_5$ integrin, identification of these biomarkers in patients remains a challenge using conventional clinical manifestation and other noninvasive testing. Therefore, it is highly demanded to develop a non-invasive approach to accurately assess the status of tumor vessels.

In our study, the tumor uptake of ^{68}Ga-NOTA-G$_3$-RGD2 and ^{68}Ga-NOTA-G$_3$-NGR2 was 6.26 ± 1.63 and 5.43 ± 2.76 % ID/g at 1 h pi, respectively ($P > 0.05$). After blocking with NOTA-G$_3$-NGR2, the tumor uptake of

^{68}Ga-NOTA-G_3-NGR2 was reduced to 1.43 ± 0.44 % ID/g at 1 h pi ($P < 0.05$). Similarly, after blocking with NOTA-G_3-RGD2, the tumor uptake of ^{68}Ga-NOTA-G_3-RGD2 was reduced to 1.28 ± 0.65 % ID/g at 1 h pi ($P < 0.05$). The successful tumor blocking of radiolabeled probes with non-radiolabeled probes suggested that both probes specifically bind to the corresponding receptors. The HT-1080 tumor uptake and targeting specificity of ^{68}Ga-NOTA-G_3-NGR2 and ^{68}Ga-NOTA-G_3-RGD2 were comparable. Although the receptors for RGD and NGR are different, our results suggest that ^{68}Ga-NOTA-G_3-NGR2 and ^{68}Ga-NOTA-G_3-RGD2 are both promising agents for imaging tumor angiogenesis with similar effects in HT-1080 tumor xenografts. In addition, our PET-CT imaging results revealed the heterogeneous expression of CD13 and $\alpha_v\beta_3/\alpha_v\beta_5$ integrin in subcutaneous HT1080 tumor xenografts. This study indicates that the detection of CD13 receptor may provide an alternative in patients with fibrosarcomas for tumor diagnosis and treatment monitoring.

Biodistribution data and PET-CT images suggest a predominant renal elimination of the probes. It was reported that proteins bind to the luminal membrane of tubular cells mainly via positively charged groups (Mogensen and Solling 1977). Several studies have shown that the renal uptake of peptides and antibody fragments is influenced by the introduction or substitution of positively- or negatively-charged groups. Decreased renal uptake without reduced tumor uptake (Miao et al. 2006; García Garayoa et al. 2008) was displayed by the substitution of a negatively charged glutamic acid residue, and increased renal accumulation (Dijkgraaf et al. 2007) was displayed by the introduction of a positively charged lysine residue into the linker of RGD moieties. To determine the charge of NGR-based probe, we loaded ^{68}Ga-NOTA-G_3-NGR2 on a strong cation exchange cartridge (Merck LiChroult SCX). The probe can be quantitatively captured by the SCX cartridge, and eluted in PBS, confirming that the probe is positively charged under the physiological condition. The rapid renal excretion of ^{68}Ga-NOTA-G_3-NGR2 may be due to the positive charges.

In our study, the targeted ligands in ^{68}Ga-NOTA-G_3-NGR2 and ^{68}Ga-NOTA-G_3-RGD2 are different whereas the linker and chelator remain the same. The cyclization of G_3-RGD2 was through the coupling of the amino group (N-terminus of phenylalanine) with the carboxyl branch in lysine residue, whereas in the case of NGR, the peptide (CNGRC) was cyclized via a disulfide bridge. The cyclization by a disulfide bridge has the advantage of simplicity as compared to amide coupling. Negussie et al. (2010) performed a study of cyclic NGR peptide coupled with thermally sensitive liposomes, and reported that the disulfide bond of cNGR might be unstable due to biodegradation. They also reported that cyclization by coupling the amino group at the N-terminus of lysine with the carboxyl branch of glutamic acid could be more robust, resulted in an enhanced binding affinity for tumor targeting applications. Contrarily, Soudy et al. (2012) reported that a cyclic NGR-containing peptide (CPNGRC, cyclized via disulfide bridge) remains an excellent binding affinity to APN, and led to a 30-fold lower IC_{50} for the inhibition of APN proteolytic activity. Nevertheless, there was no significant difference between two probes in terms of binding affinity in our study. Although both probes in this study exhibited favorable pharmacokinetics (PK), such as slow washout in tumor, rapid clearance from the blood, and low uptake in the major organs (Tanaka and Fukase 2008), additional modification of chemical structure can be performed to further optimize the PK.

It is now generally accepted that if only one molecule is blocked in tumor progression, tumors may use other alternatives. Therefore, the requirement for multi-targeted probes and/or cocktails of antiangiogenic drugs has been proposed. Our study demonstrated that NGR- and RGD-based probes were both promising agents for tumor angiogenesis imaging in HT-1080 tumor xenografts, which encourages us to construct a dual-targeting probe containing both NGR and RGD motifs. This strategy may further improve current PET images in tumors that co-express CD13 and integrin $\alpha_v\beta_3/\alpha_v\beta_5$.

Conclusion

In this study, we compared ^{68}Ga-NOTA-G_3-NGR2 and ^{68}Ga-NOTA-G_3-RGD2 probes to determine their abilities of noninvasively imaging angiogenesis in HT-1080 tumor xenografts using microPET imaging. Our results demonstrated that both probes exerted similar effects in this regard. The low liver uptake and rapid renal excretion of these two probes facilitated their clinical translation. In future studies, RGD- and NGR-based probes could be labeled with other therapeutic radionuclides for tumor treatment. A dual targeting probe containing NGR and RGD motifs may be applied for simultaneously imaging both CD13 and integrin receptors.

Acknowledgments We thank Dr. Xiaoyuan Chen (National Institute of Biomedical Imaging and Bioengineering, Bethesda, MD, USA) for his generous gift of the NOTA-G_3-RGD2 peptide. This work was supported by the USC Department of Radiology, the National Natural Science Foundation of China (Grant Nos. 81230033, 81227901, 81090270, 81371594), the National Basic Research Program of China (973 Program) (Grant No. 2011CB707704), and the International Cooperation Program of Xijing Hospital (Grant No. XJZT13G02).

Conflict of interest The authors declare that they have no conflict of interest.

References

Arap W, Pasqualini R, Ruoslahti E (1998) Cancer treatment by targeted drug delivery to tumor vasculature in a mouse model. Science 279(5349):377–380

Beer AJ, Lorenzen S, Metz S, Herrmann K, Watzlowik P, Wester HJ, Peschel C, Lordick F, Schwaiger M (2008) Comparison of integrin $\alpha_v\beta_3$ expression and glucose metabolism in primary and metastatic lesions in cancer patients: a PET study using ^{18}F-galacto-RGD and ^{18}F-FDG. J Nucl Med 49(1):22–29

Bhagwat SV, Lahdenranta J, Giordano R, Arap W, Pasqualini R, Shapiro LH (2001) CD13/APN is activated by angiogenic signals and is essential for capillary tube formation. Blood 97(3):652–659

Carmeliet P, Jain RK (2000) Angiogenesis in cancer and other diseases. Nature 407(6801):249–257

Chen K, Ma W, Li G, Wang J, Yang W, Yap LP, Hughes LD, Park R, Conti PS (2013) Synthesis and evaluation of 64Cu-labeled monomeric and dimeric NGR peptides for microPET imaging of CD13 receptor expression. Mol Pharm 10(1):417–427

Correia JD, Paulo A, Raposinho PD, Santos I (2011) Radiometallated peptides for molecular imaging and targeted therapy. Dalton Trans 40(23):6144–6167

Dijkgraaf I, Liu S, Kruijtzer JA, Soede AC, Oyen WJ, Liskamp RM, Corstens FH, Boerman OC (2007) Effects of linker variation on the in vitro and in vivo characteristics of an ^{111}In-labeled RGD peptide. Nucl Med Biol 34(1):29–35

Dirksen A, Langereis S, de Waal BF, van Genderen MH, Meijer EW, de Lussanet QG, Hackeng TM (2004) Design and synthesis of a bimodal target-specific contrast agent for angiogenesis. Org Lett 6(26):4857–4860

Faintuch BL, Oliveira EA, Targino RC, Moro AM (2014) Radiolabeled NGR phage display peptide sequence for tumor targeting. Appl Radiat Isot 86C:41–45

García Garayoa E, Schweinsberg C, Maes V, Brans L, Bläuenstein P, Tourwe DA, Schibli R, Schubiger PA (2008) Influence of the molecular charge on the biodistribution of bombesin analogues labeled with the [^{99m}Tc(CO)$_3$]-core. Bioconjug Chem 19(12):2409–2416

Goggi JL, Bejot R, Moonshi SS, Bhakoo KK (2013) Stratification of ^{18}F-labeled PET imaging agents for the assessment of antiangiogenic therapy responses in tumors. J Nucl Med 54(9):1630–1636

Haubner R, Weber WA, Beer AJ, Vabuliene E, Reim D, Sarbia M, Becker KF, Goebel M, Hein R, Wester HJ, Kessler H, Schwaiger M (2005) Noninvasive visualization of the activated $\alpha_v\beta_3$ integrin in cancer patients by positron emission tomography and [^{18}F] Galacto-RGD. PLoS Med 2 (3):e70

Jain RK, Duda DG, Willett CG, Sahani DV, Zhu AX, Loeffler JS, Batchelor TT, Sorensen AG (2009) Biomarkers of response and resistance to antiangiogenic therapy. Nature Rev Clin Oncol 6(6):327–338

Jiang W, Jin G, Ma D, Wang F, Fu T, Chen X, Chen X, Jia K, Marikar FM, Hua Z (2012) Modification of cyclic NGR tumor neovasculature-homing motif sequence to human plasminogen kringle 5 improves inhibition of tumor growth. PLoS One 7(5):e37132

Josephson L, Rudin M (2013) Barriers to clinical translation with diagnostic drugs. J Nucl Med 54(3):329–332

Kim J, Nam HY, Kim TI, Kim PH, Ryu J, Yun CO, Kim SW (2011) Active targeting of RGD-conjugated bioreducible polymer for delivery of oncolytic adenovirus expressing shRNA against IL-8 mRNA. Biomaterials 32(22):5158–5166

Li ZB, Chen K, Chen X (2008) ^{68}Ga-labeled multimeric RGD peptides for microPET imaging of integrin $\alpha_v\beta_3$ expression. Eur J Nucl Med Mol Imaging 35(6):1100–1108

Liu Z, Niu G, Shi J, Liu S, Wang F, Liu S, Chen X (2009) ^{68}Ga-labeled cyclic RGD dimers with Gly3 and PEG4 linkers: promising agents for tumor integrin $\alpha_v\beta_3$ PET imaging. Eur J Nucl Med Mol Imaging 36(6):947–957

Liu Z, Huang J, Dong C, Cui L, Jin X, Jia B, Zhu Z, Li F, Wang F (2012) ^{99m}Tc-labeled RGD-BBN peptide for small-animal SPECT/CT of lung carcinoma. Mol Pharm 9(5):1409–1417

Ma W, Kang F, Wang Z, Yang W, Li G, Ma X, Li G, Chen K, Zhang Y, Wang J (2013) ^{99m}Tc-labeled monomeric and dimeric NGR peptides for SPECT imaging of CD13 receptor in tumor-bearing mice. Amino acids 44(5):1337–1345

Miao Y, Fisher DR, Quinn TP (2006) Reducing renal uptake of ^{90}Y- and ^{177}Lu-labeled alpha-melanocyte stimulating hormone peptide analogues. Nucl Med Biol 33(6):723–733

Mogensen CE, Solling SK (1977) Studies of renal tubular absorption: partial and near complete inhibition by certain amino acids. Scand J Clin Lab Invest 37(6):477–486

Negussie AH, Miller JL, Reddy G, Drake SK, Wood BJ, Dreher MR (2010) Synthesis and in vitro evaluation of cyclic NGR peptide targeted thermally sensitive liposome. J Controlled Release 143(2):265–273

Oliveira EA, Faintuch BL, Nunez EG, Moro AM, Nanda PK, Smith CJ (2012) Radiotracers for different angiogenesis receptors in a melanoma model. Melanoma Res 22(1):45–53

Parker D (1990) Tumor targeting with radiolabeled macrocycle-antibody conjugates. Chem Soc Rev 19(3):271–291

Pasqualini R, Koivunen E, Ruoslahti E (1995) A peptide isolated from phage display libraries is a structural and functional mimic of an RGD-binding site on integrins. J Cell Biol 130(5):1189–1196

Pasqualini R, Koivunen E, Kain R, Lahdenranta J, Sakamoto M, Stryhn A, Ashmun RA, Shapiro LH, Arap W, Ruoslahti E (2000) Aminopeptidase N is a receptor for tumor-homing peptides and a target for inhibiting angiogenesis. Cancer Res 60:722–727

Ribatti D, Ranieri G, Basile A, Azzariti A, Paradiso A, Vacca A (2012) Tumor endothelial markers as a target in cancer. Expert Opin Ther Targets 16(12):1215–1225

Riss PJ, Burchardt C, Roesch F (2011) A methodical ^{68}Ga-labelling study of DO2A-(butyl-L-tyrosine)2 with cation-exchanger post-processed ^{68}Ga: practical aspects of radiolabelling. Contrast Media Mol Imaging 6(6):492–498

Roesch F, Riss PJ (2010) The renaissance of the ^{68}Ge/^{68}Ga radionuclide generator initiates new developments in ^{68}Ga radiopharmaceutical chemistry. Curr Top Med Chem 10(16):1633–1668

Schnell O, Krebs B, Carlsen J, Miederer I, Goetz C, Goldbrunner RH, Wester HJ, Haubner R, Pöpperl G, Holtmannspötter M, Kretzschmar HA, Kessler H, Tonn JC, Schwaiger M, Beer AJ (2009) Imaging of integrin $\alpha_v\beta_3$ expression in patients with malignant glioma by [^{18}F] Galacto-RGD positron emission tomography. Neuro Oncol 11(6):861–870

Shamay Y, Shpirt L, Ashkenasy G, David A (2014) Complexation of cell-penetrating peptide-polymer conjugates with polyanions controls cells uptake of HPMA copolymers and anti-tumor activity. Pharm Res 31(3)768–769

Soudy R, Ahmed S, Kaur K (2012) NGR peptide ligands for targeting CD13/APN identified through peptide array screening resemble fibronectin sequences. ACS Comb Sci 14(11):590–599

Tanaka K, Fukase K (2008) PET (positron emission tomography) imaging of biomolecules using metal-DOTA complexes: a new collaborative challenge by chemists, biologists, and physicians for future diagnostics and exploration of in vivo dynamics. Org Biomol Chem 6(5):815–828

Wang RE NY, Wu H, Hu Y, Cai J (2012) Development of NGR-based anti-cancer agents for targeted therapeutics and imaging. Anti-cancer Agents Med Chem 12(1):76–86

Wickstrom M, Larsson R, Nygren P, Gullbo J (2011) Aminopeptidase N (CD13) as a target for cancer chemotherapy. Cancer Sci 102(3):501–508

Zeglis B, Lewis JS (2011) A practical guide to the construction of radiometallated bioconjugates for positron emission tomography. Dalton Trans 40:6168–6195

Zhang J, Lu X, Wan N, Hua Z, Wang Z, Huang H, Yang M, Wang F (2014) ^{68}Ga-DOTA-NGR as a novel molecular probe for APN-positive tumor imaging using microPET. Nucl Med Biol 41(3):268–275